IEEE Access
Multidisciplinary | Rapid Review | Open Access Journal

Received April 29, 2021, accepted May 7, 2021, date of publication May 10, 2021, date of current version May 19, 2021.

Digital Object Identifier 10.1109/ACCESS.2021.3078825

Recent Approach Based Movable Damped Wave Algorithm for Designing Fractional-Order PID Load Frequency Control Installed in Multi-Interconnected Plants With Renewable Energy

AHMED FATHY[1,2] AND ABDULLAH G. ALHARBI[1], (Member, IEEE)
[1]Electrical Engineering Department, Faculty of Engineering, Jouf University, Sakaka 72388, Saudi Arabia
[2]Electrical Power and Machine Department, Faculty of Engineering, Zagazig University, Zagazig 44519, Egypt

Corresponding author: Ahmed Fathy (afali@zu.edu.eg)

The authors extend their appreciation to the Deputyship for Research & Innovation, Ministry of Education in Saudi Arabia for funding this research work through the project number 375213500.

ABSTRACT In multi-interconnected power system, keeping the changes in frequencies and tie-line powers at their specified values is vital process especially during operation under load disturbance. This target can be achieved by installing load frequency control (LFC), the main object of LFC is damping the deviations of frequencies and tie-line powers to zero. This paper proposes a new approach incorporated recent optimizer of movable damped wave algorithm (MDVA) to identify the unknown parameters of LFC represented by fractional-order proportional integral derivative (FOPID). FOPID controller is selected as it has better and robust performance, the controller is installed in multi-interconnected system with multi-sources considering renewable energy-based plants. Minimizing the integral time absolute error (ITAE) of the change in frequencies and tie-line powers is the main target. Two power systems are considered in this work, the first one comprises photovoltaic (PV) and thermal generating units while the second system includes four plants of PV, wind turbine (WT), and two thermal based plants. Moreover, the generation rate constraints and governor dead-band of thermal plant are considered. Different load disturbances in both studied systems are investigated and the obtained results via the proposed DMVA are compared to coronavirus herd immunity optimizer (CHIO), antlion optimizer (ALO), sooty tern optimization algorithm (STOA), manta ray foraging optimizer (MRFO), and sin-cos algorithm (SCA). Regarding the two-interconnected system, the proposed DMVA succeeded in achieving the best ITAE of 6.3911 during 10% disturbance applied on PV plant. Regarding to the multi-interconnected system, the best (minimum) fitness function is 0.015029 achieved via the proposed DMVA at 1% load disturbance on the first area. The results confirmed the robustness of the proposed algorithm in solving the LFC parameter estimation.

INDEX TERMS Load frequency control, fractional PID-controller, multi-interconnected system, renewable energy.

I. INTRODUCTION

The stability of power system operation is a vital issue that should be considered especially in case of sudden load disturbances. In such case, the power network frequency is affected by load disturbance and the reactive power is less affected by this violation. It is important to retain the frequency to its steady-state as fast as possible, this helps in achieving reliable operation of the network. The reliability of power system can be enhanced by interconnection with other plants, this helps in minimizing the load curtailment and guarantees continuity of the service especially in case of generation deficiency at any plant. Load frequency control (LFC) is mandatory for good management of network operation, it is responsible for keeping the frequency and tie-line loading at their specified limits during load disturbance [1]. In multi-interconnected system, the installation of such controller is important to vanish the change

The associate editor coordinating the review of this manuscript and approving it for publication was Bijoy Chand Chatterjee.

of frequencies and tie-line powers happened due to load disturbance.

Many researchers presented various design approaches for LFC, Xu *et al.* [2] designed LFC installed in multi-areas in micro grid (MG) using artificial sheep algorithm (ASA). Moreover, energy storage technology based on pumped hydropower was introduced. Tungadio *et al.* [3] reviewed many works that have been conducted in simulating LFC, the authors considered traditional, hybrid, and predictive controllers with clarifying the merits and defects of each one. Yousri *et al.* [4] employed a methodology based on Harris hawks optimizer (HHO) to estimate the proportional-integral (PI) controller based LFC parameters. Renewable energy-based plants are considered in the constructed system. Yan *et al.* [5] presented a model free approach for LFC which is available for uncertainties of renewable energy with the aid of deep reinforcement learning to minimize the frequency deviation. Amano *et al.* [6] presented an area control error (ACE) assignment to simulate LFC and battery energy storage system installed with large-scale renewable energy system. Datta *et al.* [7] presented PI and proportional-integral-derivative (PID) controllers based LFC installed in interconnected network with renewable energy sources (RESs). The constructed system composed wind, solar, and micro hydro power-based plants. Moreover, the constructed LFC was studied via controlling the ballast load. Yang *et al.* [8] developed a predictive control based LFC installed in microgrid (MG) with electric vehicles (EVs), distributed generators (DGs), and wind farm. Ali *et al.* [9] presented an approach based on coefficient diagram method for designing heat pump and EV for minimizing the fluctuation of the isolated power system frequency in case of renewable energy uncertainties. Diesel generator and renewable photovoltaic (PV) are considered as the main sources of the system. Trip *et al.* [10] introduced distributed optimal LFC for regulating the frequency and achieving economic dispatch based on derived incremental passivity for nonlinear structure. Moreover, the turbine-governor was simulated via first and second order dynamics. Khooban *et al.* [11] presented an adaptive fractional Fuzzy-PID based LFC for isolated microgrids. Moreover, EVs and batteries are considered. Furthermore, the parameters of the constructed controller were adapted using modified black hole optimizer. Çam *et al.* [12] presented two models of LFC using conventional PI and Fuzzy-PI controllers installed in single and two-interconnected systems with hydroelectric plants. Moreover, comparison between the two presented models has been conducted. Safari *et al.* [13] presented PID based LFC installed in MG with EVs, the parameters of controller were determined using artificial neural network (ANN) optimized via particle swarm optimizer (PSO). Mi *et al.* [14] designed LFC using decentralized sliding mode strategy for multi-interconnected system. An adaptive sliding mode control (SMC) was employed for simulating LFC [15]. Additionally, the disturbances and uncertainties were adapted based on adaptive dynamic programming to achieve extra control signal. Dreidy *et al.* [16] reviewed many techniques used to control the frequency of solar PV system and variable speed WT. An adaptive Fuzzy controller based LFC was constructed in [17] to minimize the frequency fluctuation and the whole cost of interconnected system. Moreover, the parameters of the presented controller have been tuned using modified PSO. The power system stabilizer for LFC was modeled and analyzed in hydro-electric power plant for damping the frequency deviation in case of load disturbance [18]. Extensive review of various approaches employed in designing LFC for deregulated power system was conducted by Pappachen *et al.* [19]. Moreover, various types of control like classical, robust, self-tunning, and soft computing were analyzed. Khooban *et al.* [20] presented SMC based LFC optimized via black hole optimizer for achieving generation/demand balance in MG with EVs. The frequency of the interconnected system including wind farm and conventional units was controlled via multi-objective PSO [21]. Fini *et al.* [22] presented multi-objective optimization problem for tunning the inertia constant, distributed energy resources' frequency droop coefficient, and LFC parameters installed in low inertia MG. A second order SMC was presented to model LFC installed in multi-interconnected based system for damping the fluctuations in frequencies and tie line powers [23]. A fractional-order based LFC installed in large electric grids with EVs and renewable energy has been presented in [24]. Moreover, the parameters of the constructed controller were determined via various evolutionary algorithms like imperialist competitive algorithm (ICA) and differential algorithm. Ko *et al.* [25] used Lyapunov theory and linear matrix inequality approach for investigating the time delays stability of LFC with penetration of EVs. PID controller optimized via the whale optimization algorithm (WOA) was presented to model LFC for interconnected system including conventional and RESs based system [26]. Ali *et al.* [27] selected a model predictive control (MPC) to represent LFC with renewable energy-based plants. The parameters of the presented controller have been optimized via sooty tern optimization algorithm (STOA) such that ITAE of change in frequencies and tie-line powers is minimized. An approach based on multi-verse optimizer (MVO) has been presented in [28] to optimize the MPC based LFC installed in large interconnected network that has RESs based plants. Fathy *et al.* [29] presented a Fuzzy-PID based LFC optimized via mine blast algorithm (MBA) installed in multi-interconnected system, the main target is to minimize the ITAE of the frequencies and tie-line powers' fluctuations during load disturbance. Moreover, GRC and GDB of reheat thermal based plants were considered. Fathy *et al.* [30] introduced an optimized adaptive neuro Fuzzy inference system (ANFIS) based LFC with the aid of antlion optimizer (ALO) for interconnected system with RESs. Prakash *et al.* [31] introduced linear quadratic regulator for PID based LFC for two-interconnected system of thermal plant with DG, solar PV and WT, and geothermal plant. Cascaded PID controllers were presented to

simulate the LFC installed in interconnected generation system [32]. Moreover, salp swarm optimizer has been used to optimize the constructed controller. Datta *et al.* [33] introduced fractional-order PID controller for simulating LFC, bacterial foraging optimizer was used to optimize the controller parameters, the constructed controller was installed in interconnected system with hybrid WT and PV based plant. Khadanga *et al.* [34] presented an approach based on sine augmented scaled SCA for designing LFC installed with multi-interconnected system. A modified fractional-order PID controller optimized via artificial ecosystem optimizer (AEO) was introduced as LFC installed in multi-interconnected system with RESs and EVs [35]. LFC based interval type-2 Fuzzy PID controller was introduced and optimized via modified equilibrium optimizer (MEO) [36]. Barakat *et al.* [37] employed HHO to optimize the parameters of PI and PD based LFC. Zhang *et al.* [38] used distributed economic MPC based LFC to achieve the desired operation of multi-interconnected system with wind plants. A Fuzzy-PID based LFC was optimized via teaching learning-based optimization (TLBO) approach [39], the designed controller was installed in electrical power system with nonlinear parameters. Sharma *et al.* [40] designed Fuzzy-PI based LFC installed in non-reheat thermal/hydro interconnected system with the aid of MVO. Arya [41] introduced a novel cascaded Fuzzy fractional-order integral derivative controller with filter installed in thermal/hydro interconnected system.

Although many works were conducted in simulating and designing the LFC in multi-interconnected-based system, most of the reported approaches required excessive effort and consumed large time in implementation. Moreover, the approaches based on metaheuristic algorithms that were employed in designing LFC lack reliability due to high probability of falling in local optima. Furthermore, a lot of these approaches required many controlling parameters that defined by the user, tunning of such parameters is still big challenge to guarantee optimum solution. Additionally, many works presented conventional types of LFC like PI, PID, and Fuzzy while presenting advanced controller like fractional-order requires more attention from researchers in this field as it is more efficient than the conventional ones. The authors considered all these defects by proposing fractional-order PID (FOPID) based LFC optimized via recent approach of movable damped wave algorithm (MDVA) and installed in multi-interconnected system with RESs. The authors selected FOPID controller as it has more adaptable response in terms of time and frequency, moreover it has better and robust performance. The DMVA is selected as it has balance between exploration and exploitation phases, this avoids stuck in local optima, moreover the algorithm is simple in implementation and less sensitive to the parameters defined by the user.

The work contributes by the following points:

- It is the first time to propose a methodology incorporated movable damped wave algorithm (MDVA) for tunning the optimal parameters of FOPID-LFC installed in two and multi-interconnected systems.
- Renewable energy-based plants like photovoltaic (PV) and wind turbine (WT) are considered.
- The generation rate constraints (GRC) and governor dead-band (GDB) of thermal-based plant are considered.
- Comparison to coronavirus herd immunity optimizer (CHIO), antlion optimizer (ALO), sooty tern optimization algorithm (STOA), manta ray foraging optimizer (MRFO), and sin-cos algorithm (SCA) is conducted.
- The robustness of the proposed FOPID-LFC is confirmed by applying different load disturbances.

The paper is organized as follows: section II presents the models of the different interconnected systems, section III introduces the principles of movable damped wave algorithm (MDVA), section IV shows the proposed solution methodology, section V presents the results and discussions, and section VI introduces the conclusions.

II. INTERCONNECTED SYSTEM MODEL

In this study, two interconnected systems are analyzed, the first one consists of photovoltaic (PV) based plant and thermal generating unit while the second system comprises four interconnected plants of PV, wind turbine (WT), and two thermal power plants with GRC and GDB. In this section, the model and block diagram of each plant are presented. Moreover, the main principle of fractional-order PID controller is presented.

A. THERMAL GENERATING UNIT MODEL

The thermal generating plant comprises generating unit, prime-mover (steam turbine), speed-governor, and reheater, the model of each component can be written as follows [42]:

$$G_g = \frac{k_g}{1 + T_g s} \tag{1}$$

$$G_t = \frac{k_t}{1 + T_t s} \tag{2}$$

$$G_r = \frac{1 + k_r T_r s}{1 + T_r s} \tag{3}$$

$$G_{gen} = \frac{k_p}{1 + T_p s} \tag{4}$$

where G_g, G_t, G_r, and G_{gen} are the governor, steam turbine, reheater, and generating unit transfer functions, k_g and T_g are the governor gain and time constant, k_t and T_t are the steam turbine gain and time constant, k_r and T_r are the reheater gain and time constant, k_p and T_p are the generating unit gain and time constant.

B. PHOTOVOLTAIC-BASED PLANT MODEL

The photovoltaic (PV) based system comprises some of solar cells that are connected in series and parallel to supply the required power to load. The PV system performance depends on the irradiance and temperature, the terminal voltage of the

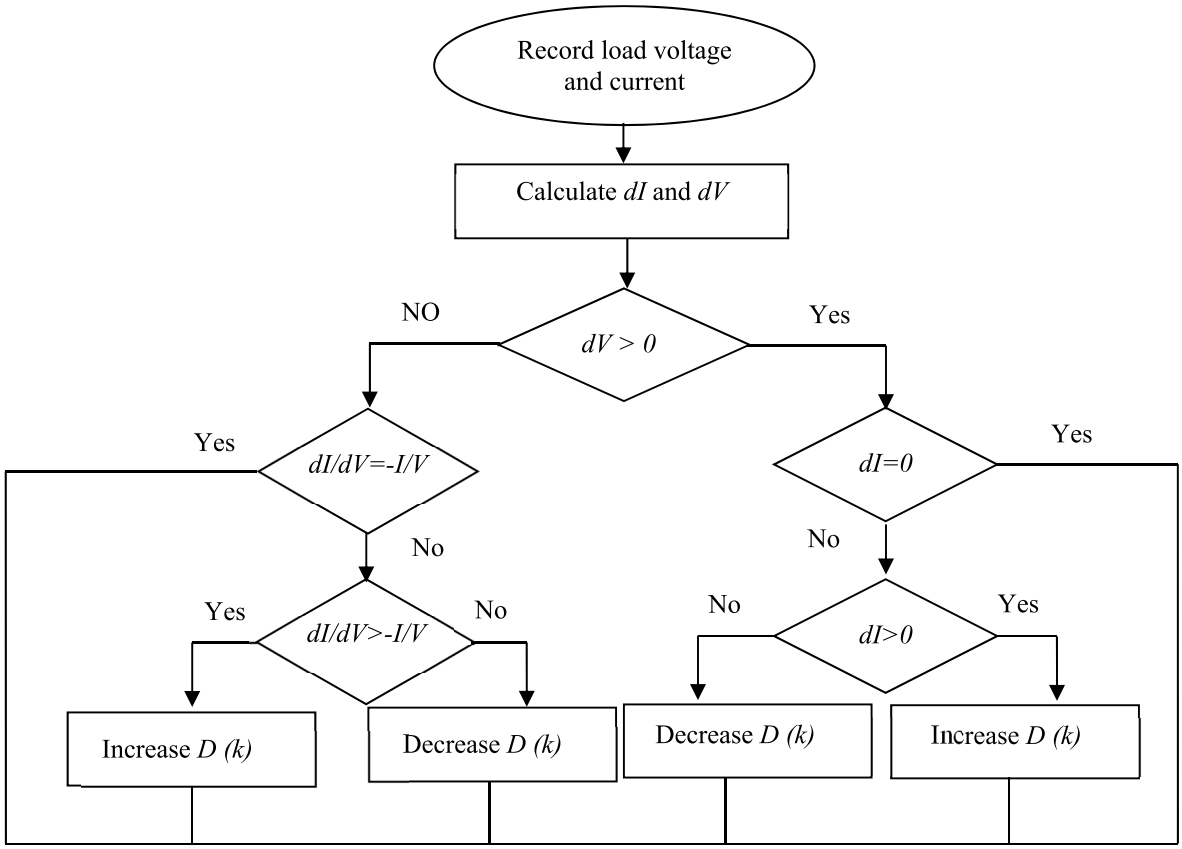

FIGURE 1. Flowchart of INC based tracker approach.

PV panel can be expressed as follows [43]:

$$V = \left(\frac{N_s \varepsilon Z T_a}{Q}\right) \ln\left[\frac{N_p G I_{ph} - I + N_p I_o}{N_p I_o}\right] - \left(\frac{N_s I R_s}{N_p}\right) \quad (5)$$

where I is the current of PV panel, Q is the electron charge, Z is the constant of Boltzmann, T_a is the temperature of PV module, N_s is the number of cells connected in series, N_p is the number of strings connected in parallel, R_s is the series resistance of PV cell, ε is the completion factor, I_{ph} is the photocurrent, I_o is the reverse saturation current, and G is the irradiance. In the voltage-power curve of the PV panel, there is only one maximum point that called maximum power point (MPP), this point is tracked with the aid of tracker [44].

There are many algorithms of maximum power point tracker (MPPT), the most popular one is incremental conductance (INC). To track the MPP, a converter is connected to the PV panel terminals and the duty cycle of its MOSFET is controlled via INC algorithm. Fig. 1 shows the flowchart of INC, in this work dc-dc buck converter is considered.

INC based approach is based on the following formula [45]:

$$\begin{cases} \frac{dP_{PV}}{dV_{PV}} > 0 & At\ right\ of\ MPP \\ \frac{dP_{PV}}{dV_{PV}} = 0 & At\ MPP \\ \frac{dP_{PV}}{dV_{PV}} < 0 & At\ left\ of\ MPP \end{cases} \quad (6)$$

The transfer functions represent the PV module can be written as follows [46]:

$$G_1 = \left(\frac{s^2}{s^2+\omega^2}\right)\left(\frac{V\left(s^2+\omega^2\right)\left(s^2+2\omega^2\right)}{ks^2\left(s^2+4\omega^2\right)}\right)\left(\frac{1-e^{-sT_s}}{sT_s}\right) \quad (7)$$

$$G_2 = \left(\frac{M_1/LC}{s^2+\left(\frac{1}{RC}\right)s+\frac{1}{LC}}\right)\left(\frac{1-e^{-sT_s/2}}{1+e^{-sT_s/2}}\right)\left(\frac{M_2}{1+sT_s}\right) \quad (8)$$

where R, L, and C are the converter output resistance, inductance, and capacitance respectively, ω is the frequency of grid, M_1 is the voltage gain of buck converter, M_2 is the voltage gain of inverter, and T_s is the sampling time.

C. WIND TURBINE-BASED PLANT MODEL

Wind turbine (WT) is considered by power coefficient (C_p) which is defined as a function of the tip speed ratio (λ) and the blade pitch angle (β). It is important to keep the tip speed ratio at its optimal value to enhance the extracted wind power. The tip speed ratio is equal to the WT angular rotor speed divided by the linear wind speed as follows [47]:

$$\lambda = \frac{\omega_t R}{V_w} \quad (9)$$

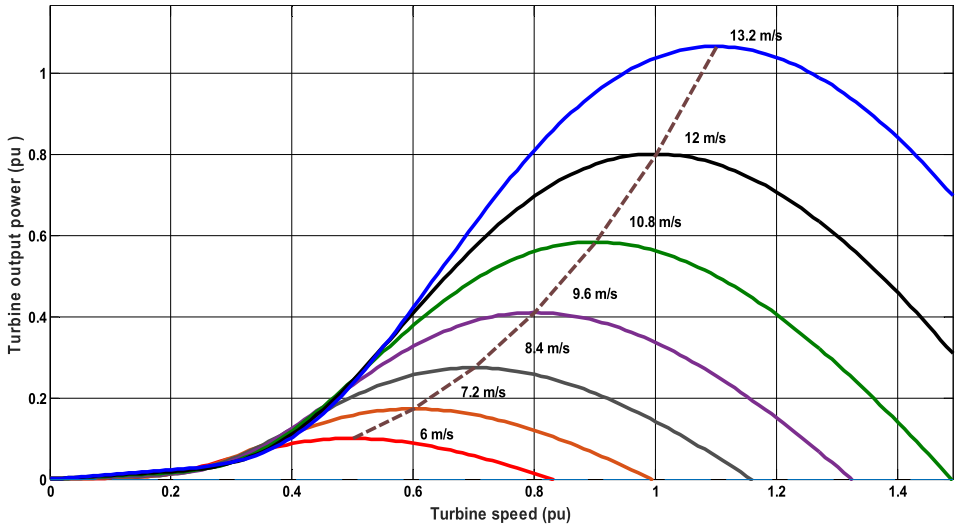

FIGURE 2. WT mechanical power versus mechanical speed at different wind speeds.

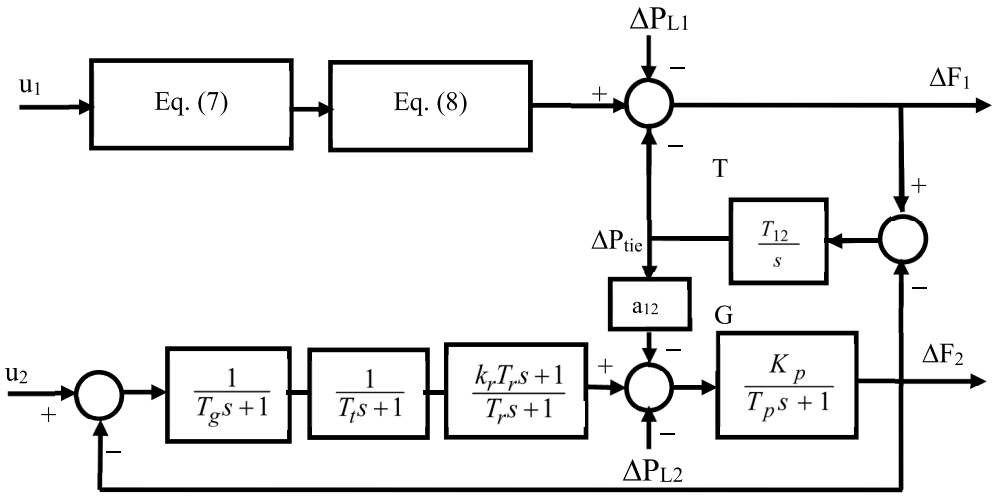

FIGURE 3. The proposed PV/thermal interconnected system.

where R is the WT rotor radius, V_w represents the wind speed, ω_t is the WT speed.

The wind power extracted from WT can be expressed as follows [48]:

$$P_W = \frac{1}{2}\rho A C_p(\lambda, \beta) V_w^3 \tag{10}$$

where ρ represents the density of air, and A is the swept area of WT blades.

The power coefficient of WT is given in the following Eq.:

$$C_p = (0.44 - 0.0167 \times \beta) \sin\left(\frac{\pi(\lambda - 2)}{15 - 0.3\beta}\right) - 0.00184(\lambda - 3)\beta \tag{11}$$

The mechanical power produced by WT can be given in the following formula [49]:

$$P_m = C_p(\lambda, \beta) P_w \tag{12}$$

The variations of WT mechanical power and mechanical speed of rotor at different wind speeds are shown in Fig. 2.

In this work, the authors analyzed two systems, the first has two interconnected plants of PV and thermal generating units, the block diagram of such system is shown in Fig. 3. The second considered system comprises four interconnected plants, PV, wind turbine, and two thermal based units with GRC and GDB, the diagram of such system is shown in Fig. 4.

D. MAIN PRINCIPLE OF FRACTIONAL-ORDER PID CONTROLLER

Fractional-order PID controller (FOPID) was introduced via *Podlubny* [50], FOPID is better than the conventional PID in term of performance especially for closed loop control systems. This controller is defined by five parameters which are the gains of PID (K_p, K_i, and K_d), the integrator order (λ),

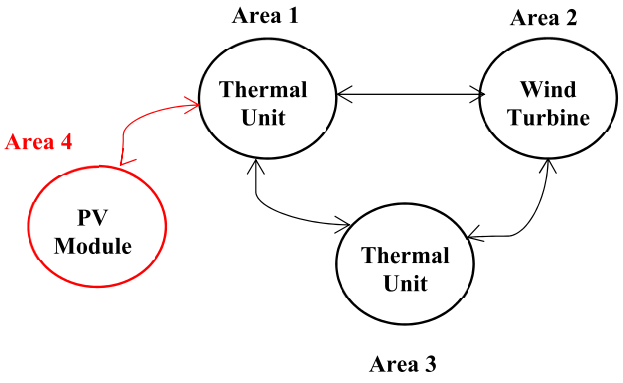

FIGURE 4. The proposed PV/WT/thermal interconnected system.

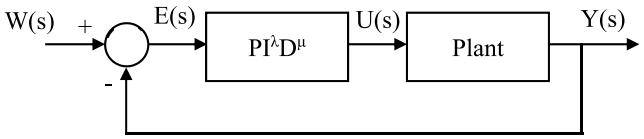

FIGURE 5. Block diagram of FOPID controller with plant.

and the derivative order (μ). The block diagram of FOPID is shown in Fig. 5, the transfer function of FOPID can be written as follows:

$$G_c(s) = K_p + \frac{K_i}{s^{\lambda}} + K_d s^{\mu} \quad \lambda, \mu \succ 0 \tag{13}$$

The output of FOPID controller can be obtained by solving Eq. (13) as follows:

$$u(t) = K_p \times e(t) + K_i \times D^{-\lambda} \times e(t) + K_d \times D^{-\mu} \times e(t) \tag{14}$$

Referring to Fig. 5, the controller is responsible for feeding the plant with the reference input such that the error, E(s), is minimized. The performance of controller gains more flexibility via tunning the parameters λ and μ. To guarantee correct tunning of the FOPID controller, metaheuristic approach of movable damped wave algorithm (MDVA) is proposed.

III. MOVABLE DAMPED WAVE ALGORITHM (MDVA)

In 2019, *Rizk-Allah et al.* [51] introduced recent metaheuristic optimization approach motivated from the waveform behavior under oscillation phenomena, it is known as movable damped wave algorithm (MDVA). The damped sin wave is defined as the wave with amplitude decreases and reaches to zero with time. The algorithm is a population-based approach that starts by initializing random solutions and the corresponding objective function for each probable solution is calculated. The obtained solution is improved with the aid of some rules which is considered as the algorithm kernel.

The formula of damped wave can be written as follows:

$$x_i^{t+1} = \left(\frac{\pm\alpha(t)}{\zeta + x_i^t}\right) \sin\left(\frac{2\pi}{\gamma}\right) x_i^t \tag{15}$$

where α is a parameter employed to change the damped wave amplitude, ζ is used to move the wave to either right side or left side, and γ is used for either contraction or expansion the damped wave. One of the strength points in DMVA is that the solution is redistributed in the search space due to the wave damped cyclic pattern, this action improves the exploration tendency. Moreover, the exploitation phase can be enhanced by permitting the wave to move around the best solution. Therefore, the damped wave updates its position based on the following formula:

$$x_{i,j}^{t+1} = \left(\frac{\alpha}{\zeta + x_{i,j}^t}\right) \sin\left(\frac{2\pi}{\gamma}\right) x_{i,j}^t + x_{best,j}, \quad i = 1, 2, \ldots, PS \tag{16}$$

where $x_{i,j}^t$ is the i^{th} solution position in j^{th} dimension at t^{th} iteration, $x_{best,j}$ is the best solution in j^{th} dimension, and PS is the size of population. The controlling parameters of DMVA are α, ζ, and γ, the first one is employed to make balance between exploration and exploitation to evaluate the recommended regions in the search space.

The parameter ζ is responsible for dictating the next horizontal movement of the wave either to the left side or to the right one while γ is used for defining the next vertical movement either up or down. These parameters are assigned randomly from the bounds of the problem therefore, the algorithm is not sensitive to confident values of these parameters. To make balance between the exploration and exploitation phases, the parameter α is adaptively varied using the following Eq.:

$$\alpha = \alpha_{\min} + (\alpha_{\max} - \alpha_{\min}) \times \left(\frac{t_{\max} - t}{t_{\max}}\right) \tag{17}$$

where α_{min} and α_{max} are constants which are assigned as 0 and 1 respectively, t_{max} is the maximum iteration, and t is the current iteration. Eq. (17) clarifies that, α has a big value at early iteration, this helps in enhancing the exploration while at the final iteration it has small value that my highlight the local exploitation. Fig. 6 shows the flowchart of DMVA.

IV. THE PROPOSED SOLUTION METHODOLOGY

The parameters of fractional-order PID controller based LFC incorporated in interconnected system are determined via a novel methodology of damped movable wave algorithm (DMVA). The integral time absolute error (ITAE) of the change in frequencies and tie-line powers is considered as the target to be minimized. While the design variables to be identified are K_p, K_i, K_d, λ, and μ, the proposed structure of the designing process is shown in Fig. 7.

The objective function considered in this work can be written as follows:

$$ITAE = \int_0^t t. \left[\sum_{i=1}^{N_{Area}} \left|\Delta F_i + \Delta P_{tie,i}\right|\right] dt \tag{18}$$

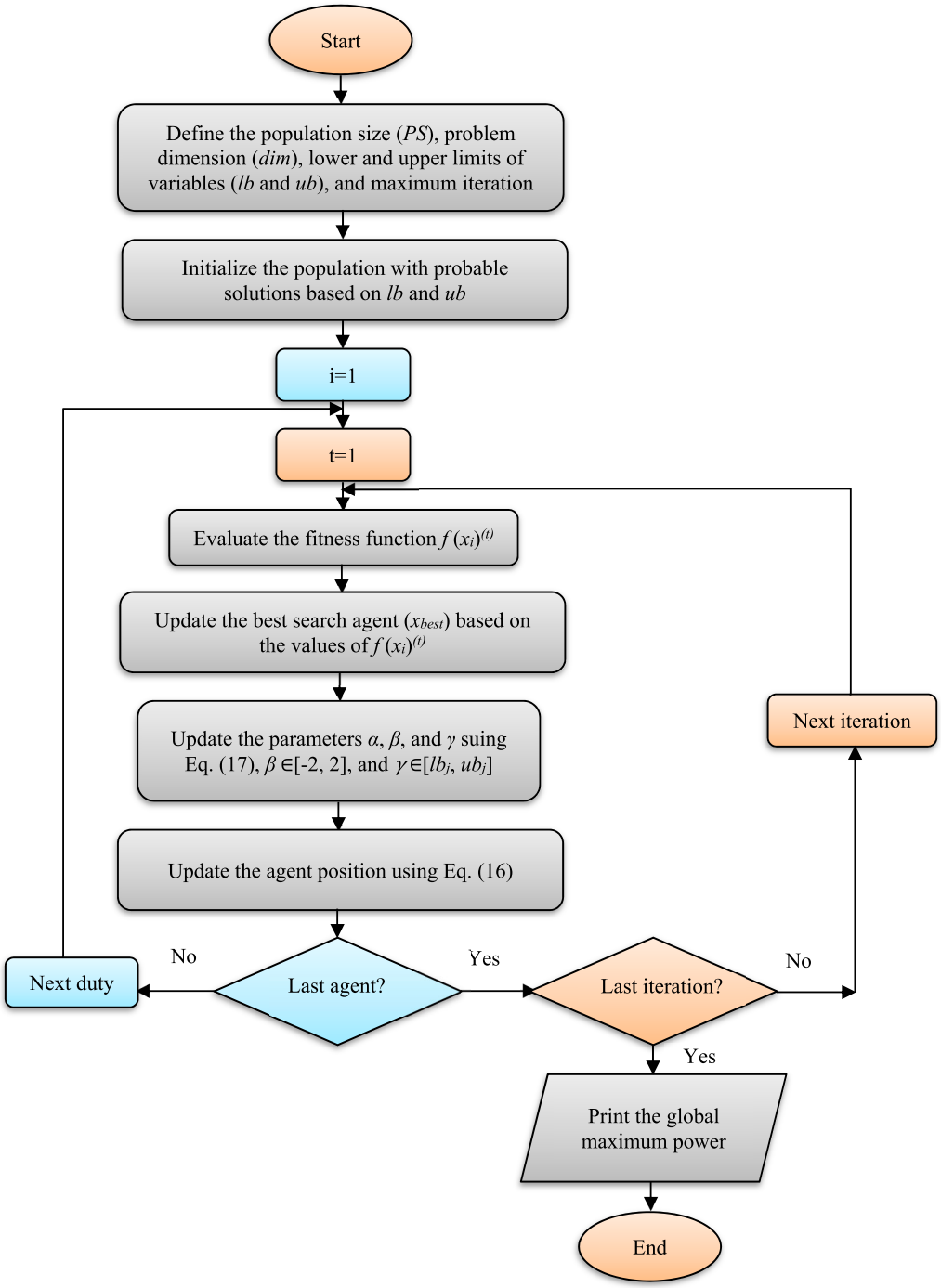

FIGURE 6. Flowchart of DMVA.

where ΔF_i is the change in frequency of i^{th} area, $\Delta P_{tie,i}$ is the change in i^{th} area tie-line power, N_{Area} is the number of connected areas, and t is the time of simulation.

The constraints considered in this work are given in Eq. (19) as follows:

$$\begin{aligned} K_{p,\min} \leq K_p \prec K_{p,\max} \\ K_{i,\min} \leq K_i \prec K_{i,\max} \\ K_{d,\min} \leq K_d \prec K_{d,\max} \\ \lambda_{\min} \leq \lambda \prec \lambda_{\max} \\ \mu^{\min} \leq \mu \prec \mu^{\max} \quad \forall i \in N_c \end{aligned} \tag{19}$$

where *max* and *min* refer to the maximum and minimum bounds of the parameters, and N_C is the number of controllers installed in the system. In this work, the minimum and maximum limits of FOPID controller's parameters are assumed to 0 and 1 respectively. The steps given in Fig. 6 are

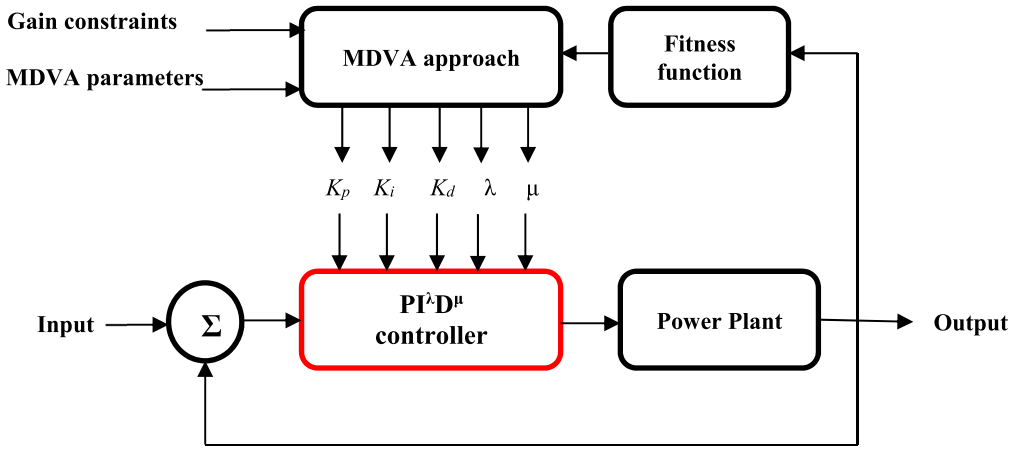

FIGURE 7. The proposed structure of FOPID-LFC controller optimized via DMVA.

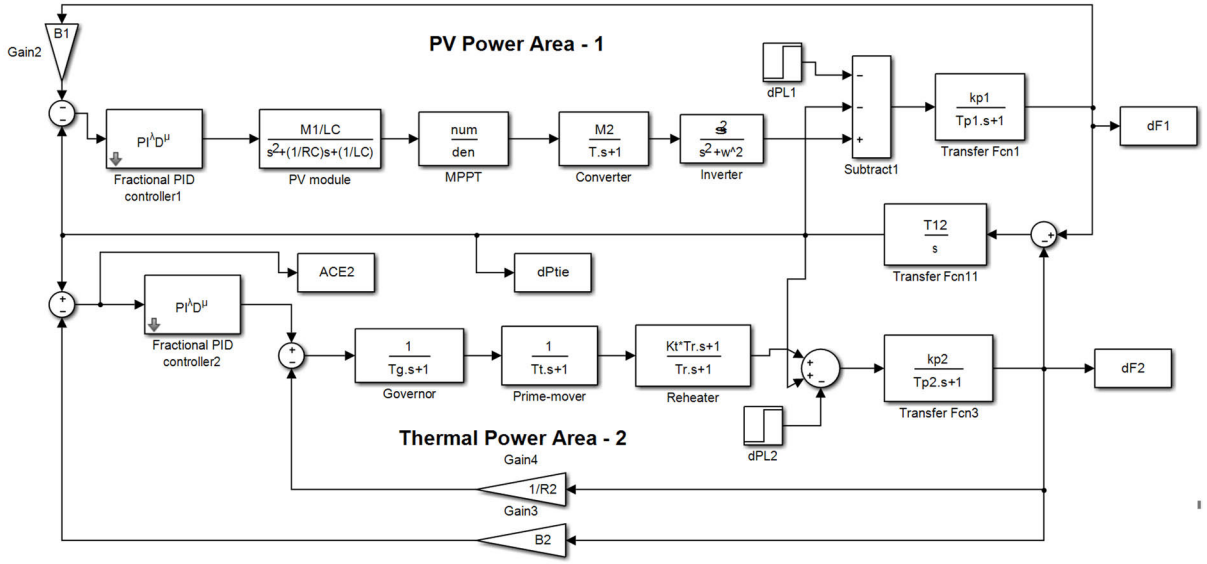

FIGURE 8. Simulink model of the proposed PV/Thermal interconnected system.

implemented with considering the fitness function given in Eq. (18) and constraints given in Eq. (19).

The proposed methodology incorporated DMVA is characterized by balance between exploration and exploitation phases, this avoids stuck in local optima. Moreover, DMVA is not sensitive to the controlling parameters. Furthermore, it is simple in construction and implementation. These features enable the proposed approach to solve many complicated problems with high-dimension.

V. RESULTS AND DISCUSSIONS

Two interconnected systems are considered in this work, the first one comprises PV based plant connected to thermal generating unit with reheater. While, the second system composes four interconnected system, PV based plant, wind turbine (WT) based plant, and two thermal generating units with GRC and GDB. Different load disturbances are considered in the analysis as described below, moreover, excessive comparison analysis to other metaheuristic optimization approaches is conducted.

A. ANALYSIS OF TWO-INTERCONNECTED SYSTEM

In this system, the PV generating unit with maximum power point tracker (MPPT) is connected to thermal generating unit with reheater. The topology of such system with the proposed FOPID controllers is built in Simulink/Matlab as shown in Fig. 8. The parameters of such system are given in [30], the capacity of PV plant is 500 kW while the thermal plant has rated power of 2000 MW with load of 50% of its rated power. The proposed MDVA is implemented for 100 iteration, 50 population size, and 10 independent runs. The first disturbance considered in such system is 10% on PV

TABLE 1. The optimal parameters of FOPID controllers at 10% load disturbance applied on PV plant.

	CHIO	ALO	STOA	MRFO	SCA	The proposed DMVA
K_{p1}	0.78754	1.000	1.000	0.99929	1.000	1.000
K_{i1}	1.000	1.000	0.96125	0.99664	1.000	0.83082
K_{d1}	1.000	1.000	1.000	0.99936	1.000	1.000
λ_1	0.66414	0.99711	0.32959	0.29312	0.50351	0.30367
μ_1	0.64915	0.58038	0.87119	0.94949	0.77449	0.93946
K_{p2}	0.32391	0.79253	0.000223	0.95183	0.000245	0.75083
K_{i2}	0.7909	0.99999	0.51324	0.45503	0.81743	1.000
K_{d2}	0.16619	0.98696	0.19783	0.013432	0.22541	0.1442
λ_2	0.60024	0.70982	0.3032	0.98155	0.000674	0.98059
μ_2	0.45231	0.99524	0.000123	0.41155	0.000377	0.02925
Elapsed time (s)	20068.283	16062.355	13983.285	14913.706	13417.439	7174.8576
Fitness function	8.6836	7.3091	7.1176	6.9375	7.4021	6.3911
IAE	7.0134	6.2793	6.7185	6.4305	6.0948	5.9883
ISE	0.1549	0.1486	0.1576	0.1475	0.1236	0.1238
ITSE	0.0444	0.0373	0.0413	0.0365	0.0318	0.0312

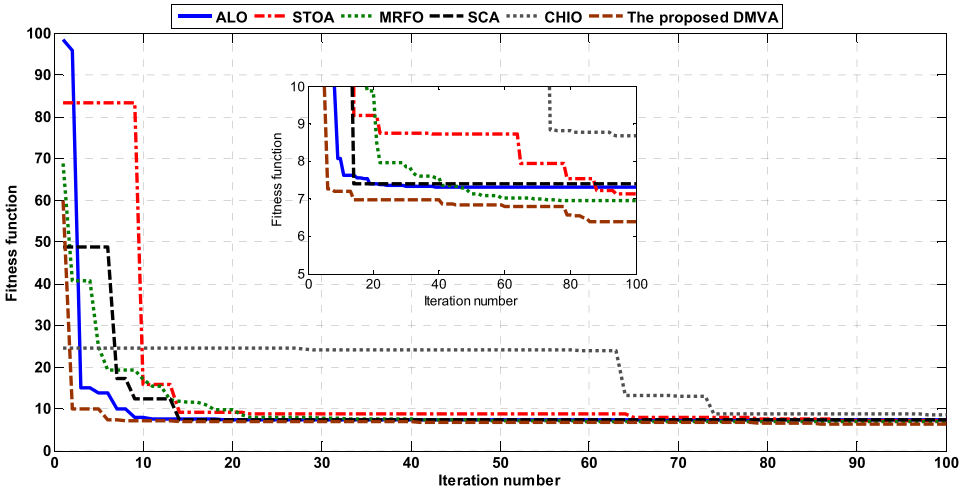

FIGURE 9. Variation of fitness function during iterative process 10% load disturbance applied on PV plant.

based plant. The proposed MDVA based approach is applied and the obtained results are compared to other approaches like coronavirus herd immunity optimizer (CHIO), antlion optimizer (ALO), sooty tern optimization algorithm (STOA), manta ray foraging optimizer (MRFO), and sin-cos algorithm (SCA). The obtained results are tabulated in Table 1, moreover the integral absolute error (IAE), integral square error (ISE), and integral time square error (ITSE) are calculated. The minimum ITAE is 6.3911 obtained via the proposed approach, the best IAE, ISE, and ITSE are 5.9883, 0.1238, and 0.0312 obtained via the proposed DMVA. Moreover, the best (minimum) elapsed time is 7174.8576 s required for implementing DMVA.

The fitness function versus the iteration number is given in Fig. 9.

The time responses of change in frequencies and tie-line powers obtained via each optimizer are shown in Fig. 10, the obtained time responses confirm the superiority of the proposed approach compared to the others.

It is important to investigate the performance of each optimizer during the implementation, this is done by calculating the statistical parameters (best, worst, mean, median, variance, and standard deviation), the obtained statistical parameters are tabulated in Table 2. The proposed approach outperformed the others achieving the best variance and standard deviation of 0.0279 and 0.1672 respectively.

Additionally, to clarify the competence of the proposed approach in solving the problem of estimating the FOPID based LFC parameters, performance specifications including rise time (t_r), settling time (t_s), minimum settling time ($t_{s,min}$), maximum settling time ($t_{s,max}$), over shoot (OS), under shoot (Us), peak value, and peak time (t_{peak}) for time responses of ΔF_1, ΔF_2, and ΔP_{tie} obtained via each optimizer are calculated and tabulated in Table 3. The obtained

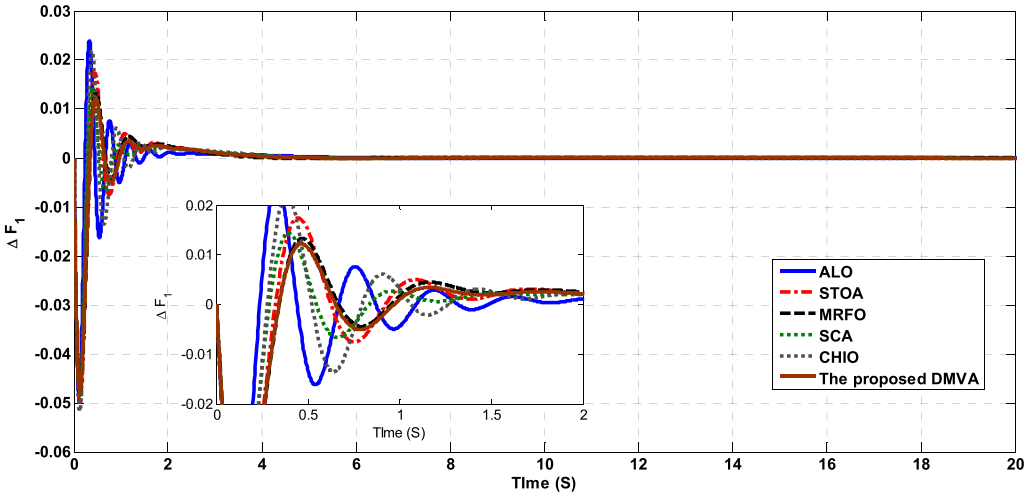

(a)

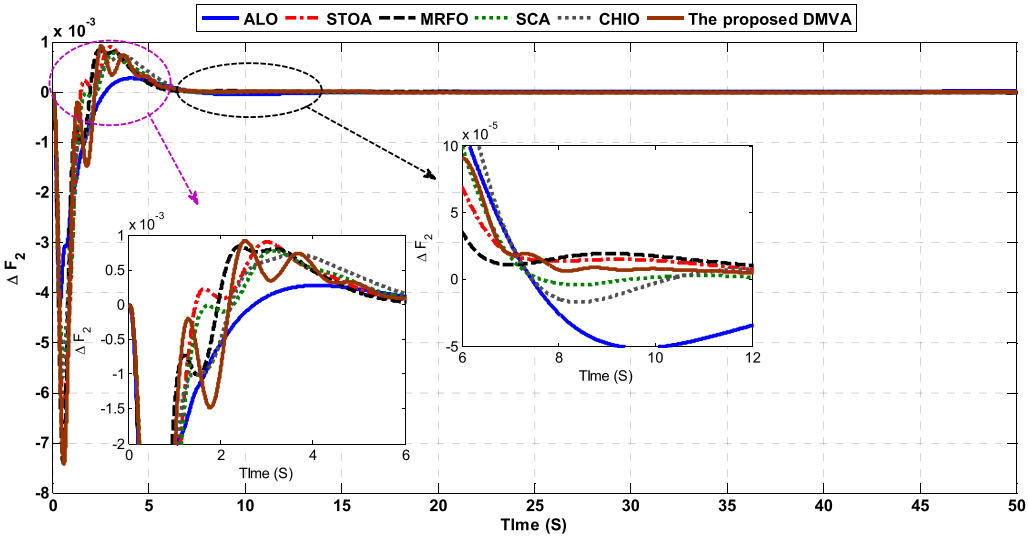

(b)

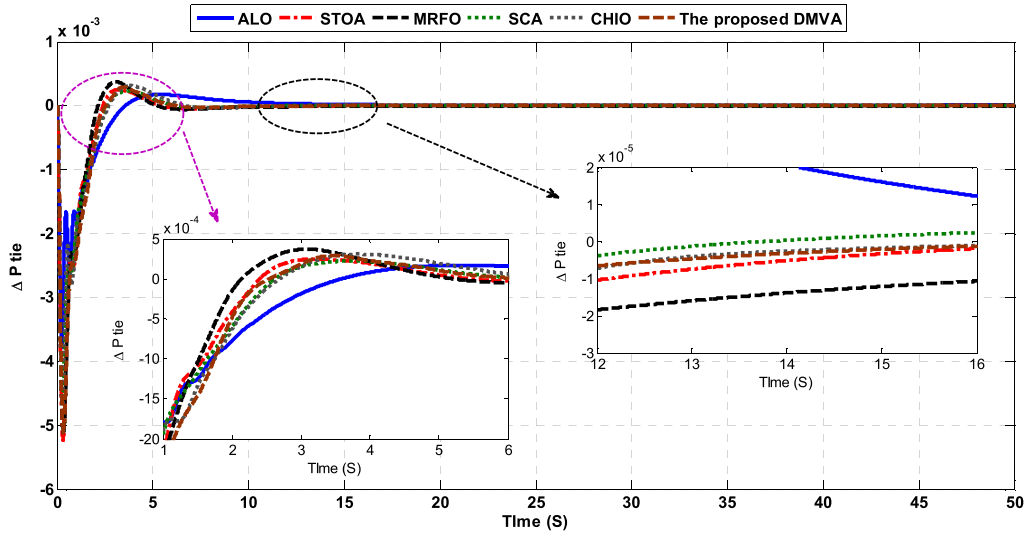

(c)

FIGURE 10. The time-responses of (a) ΔF_1, (b) ΔF_2, and (c) ΔP_{tie} for 10% load disturbance applied on PV plant.

TABLE 2. Statistical parameters of the proposed DMVA in comparison to the others at 10% load disturbance applied on PV plant.

	CHIO	ALO	STOA	MRFO	SCA	The proposed DMVA
Best	8.6836	7.30911	7.11756	6.9375	7.40211	6.3911
Worst	413.15	11.7457	8.51902	8.5609	235.974	6.9334
Mean	58.936	8.33968	7.87233	7.6008	76.4518	6.5623
Median	14.639	7.77655	7.96488	7.5137	8.58249	6.5108
Variance	15631.25	1.73189	0.22223	0.3195	12117.98	0.0279
Standard deviation	125.0250	1.31602	0.47142	0.5653	110.0817	0.1672

TABLE 3. Performance specifications of frequencies and tie-line powers' deviations at 10% load disturbance applied on PV plant.

	t_r (s)	t_s (s)	$t_{s,min}$ (s)	$t_{s,max}$ (s)	Os (Hz)	Us (Hz)	Peak (Hz)	t_{peak} (s)
Change in frequency of area 1 (ΔF_1)								
CHIO	1.5609e-06	3.4180	-0.0518	0.0218	4.4248e-02	1.8648e-02	0.0518	0.1227
ALO	1.0011e-06	3.1316	-0.0477	0.0122	6.3471e-02	1.6234e-03	0.0477	0.1261
STOA	2.1532e-06	3.0758	-0.0505	0.0174	3.1251e-02	1.0788e-02	0.0505	0.1299
MRFO	3.5572e-06	2.9620	-0.0477	0.0133	1.7886e-02	4.9806e-02	0.0477	0.1282
SCA	2.9871e-06	3.2744	-0.0485	0.0144	2.1628e-02	6.4296e-02	0.0485	0.1168
The proposed DMVA	5.4466e-08	2.5379	-0.0162	0.0239	7.2883e-03	1.4861e-04	0.0487	0.1112
Change in frequency of area 2 (ΔF_2)								
CHIO	0.0088	6.2744	-0.0057	7.2459e-04	5.0521e-02	6.4195e-01	0.0057	0.5041
ALO	0.0074	5.4501	-0.0074	9.1869e-04	1.0244e-03	1.2664e-02	0.0074	0.5828
STOA	0.0097	5.4874	-0.0063	8.9894e-04	4.0677e-02	5.7704e-01	0.0063	0.5717
MRFO	0.0115	5.1213	-0.0074	8.3494e-04	2.8531e-02	3.2302e-01	0.0074	0.5470
SCA	0.0108	5.9702	-0.0053	7.7723e-04	2.4730e-02	3.6089e-01	0.0053	0.5813
The proposed DMVA	6.4194e-05	6.3213	-5.1437e-05	2.7445e-04	6.8731e-02	1.0568e-04	0.0042	0.3832
Change in tie-line power (ΔP_{tie})								
CHIO	0.0014	5.7005	-4.3611e-05	3.0818e-04	3.0676e-01	4.7037e-02	0.0047	0.2722
ALO	0.0012	5.0029	-2.8585e-05	2.8933e-04	4.6973e-01	8.3216e-02	0.0051	0.3218
STOA	0.0013	4.5821	-4.9547e-05	2.4696e-04	1.8580e-01	3.9607e-02	0.0052	0.3105
MRFO	0.0020	4.5269	-6.1270e-05	3.7051e-04	1.6981e-01	2.3693e-02	0.0051	0.3220
SCA	0.0024	5.1689	-3.4016e-05	2.2329e-04	1.2011e-01	2.4363e-02	0.0045	0.2787
The proposed DMVA	2.3800e-04	8.8779	-2.6890e-07	1.7164e-04	2.4108e-02	5.3285e-03	0.0038	0.2328

TABLE 4. The optimal parameters of FOPID controllers at 10% load disturbance applied on thermal plant.

	CHIO	ALO	ST OA	MRFO	SCA	The proposed DMVA
K_{p1}	0.17448	0.88101	0.23463	0.0019354	0.11943	1.000
K_{i1}	0.18844	0.92065	0.000	0.29759	0.43727	1.000
K_{d1}	0.94297	0.89986	0.000	0.17374	0.20853	1.000
λ_1	0.6238	0.67541	0.12352	0.69427	0.92522	1.000
μ_1	0.61024	0.92672	0.91571	0.93558	0.93146	1.000
K_{p2}	0.53212	0.76139	0.82806	0.95313	0.83196	0.40973
K_{i2}	0.66787	0.93786	0.86401	0.96173	0.90409	1.000
K_{d2}	0.83942	0.88993	0.93867	0.86302	0.90012	0.87697
λ_2	0.1944	0.73149	1.000	0.27029	0.36282	1.000
μ_2	0.95077	0.00074931	0.000	0.30964	0.58075	0.000
Fitness function	23.95017	11.25177	6.81865	8.02517	10.66431	1.205898

performance specifications confirm the superiority of the proposed approach compared to the others. It is clear that, the results obtained during 10% load disturbance on PV based plant confirmed the competence and reliability of the proposed approach incorporated DMVA in solving the handled optimization problem.

The second disturbance considered in PV/thermal interconnected system is 10% on thermal generating unit.

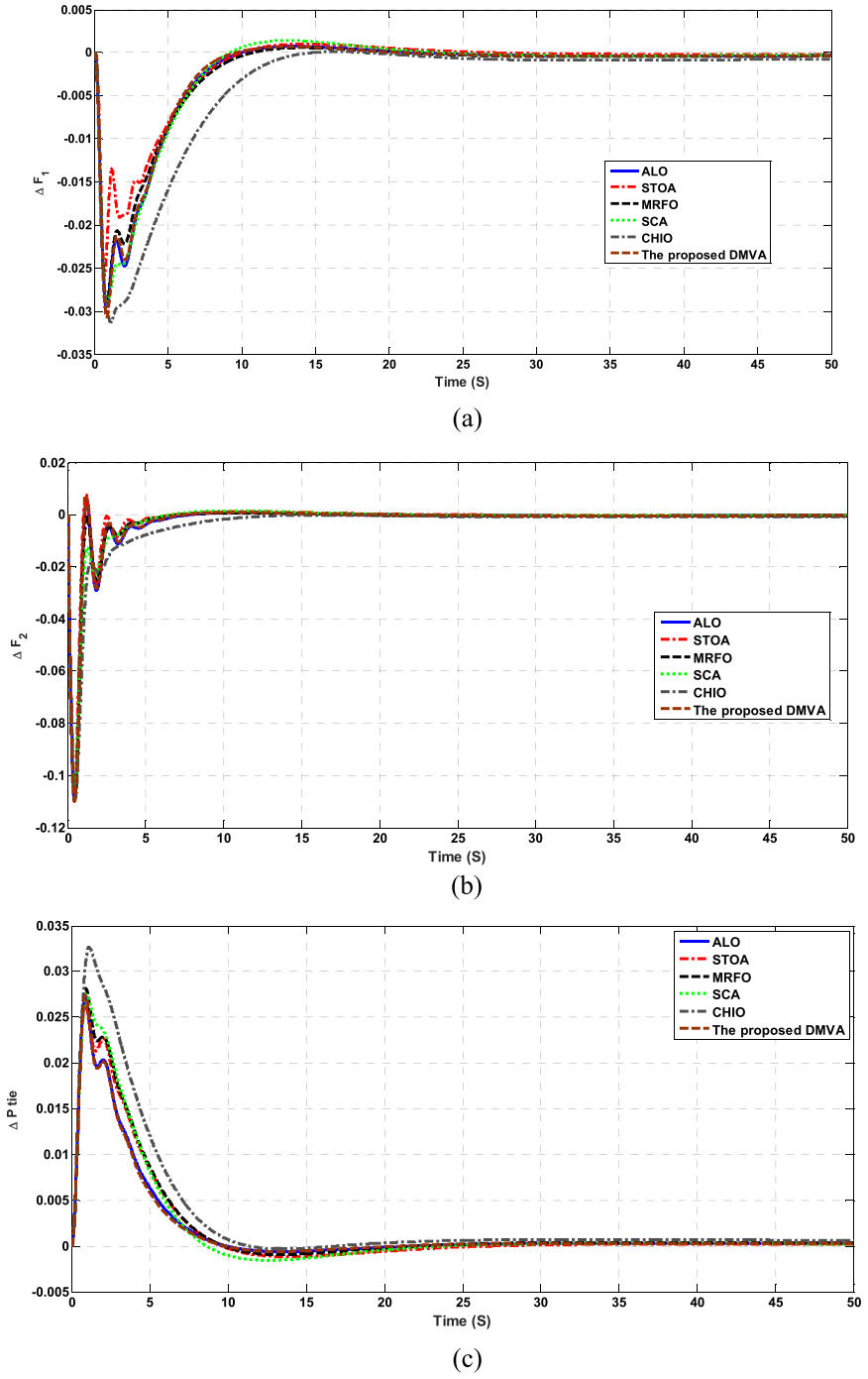

FIGURE 11. The time-responses of (a) ΔF_1, (b) ΔF_2, and (c) ΔP_{tie} for 10% load disturbance applied on thermal plant.

The optimal parameters of FOPID-LFC controllers are given in Table 4. The proposed DMVA comes in the first rank achieving the best fitness function of 1.205898 while CHIO comes in the last rank with ITAE of 23.95017. The time responses of ΔF_1, ΔF_2, and ΔP_{tie} in such case are shown in Fig. 11, the proposed DMVA achieved good performance for two interconnected PV/thermal system during the second load disturbance.

Finally, one can get that the proposed approach incorporated DMVA is efficient in identifying the optimal parameters FOPID based LFC installed in PV/thermal interconnected system operated at different load disturbances.

B. ANALYSIS OF FOUR-INTERCONNECTED SYSTEM

Recently, the generating units in most power system are not limited to one type but rather include different types such as

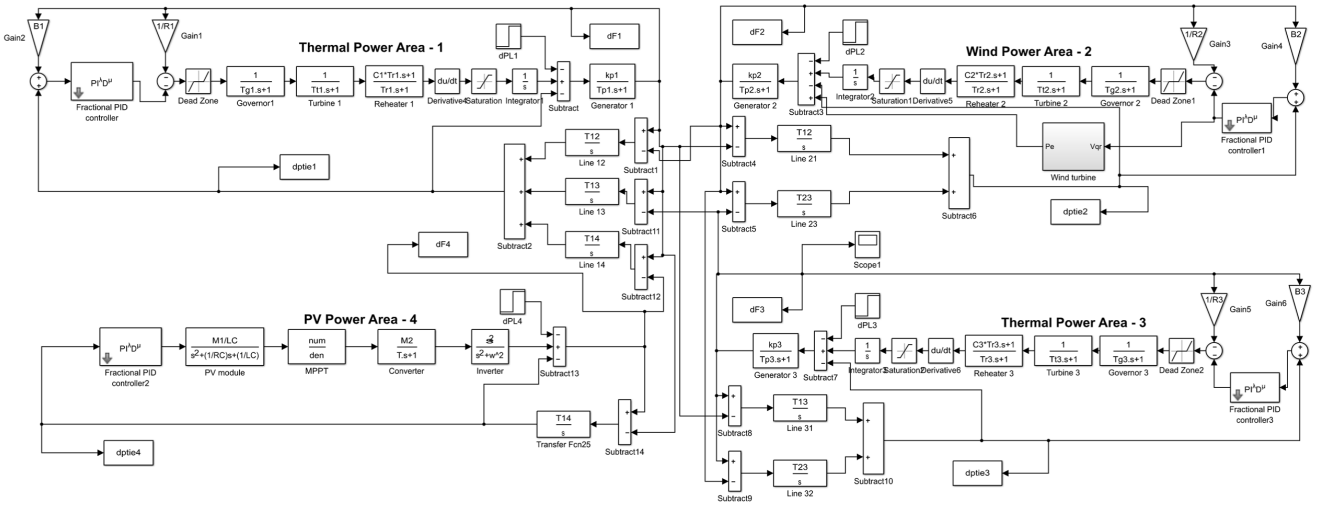

FIGURE 12. Simulink model of the proposed PV/WT/Thermal interconnected system considering GRC and GDB.

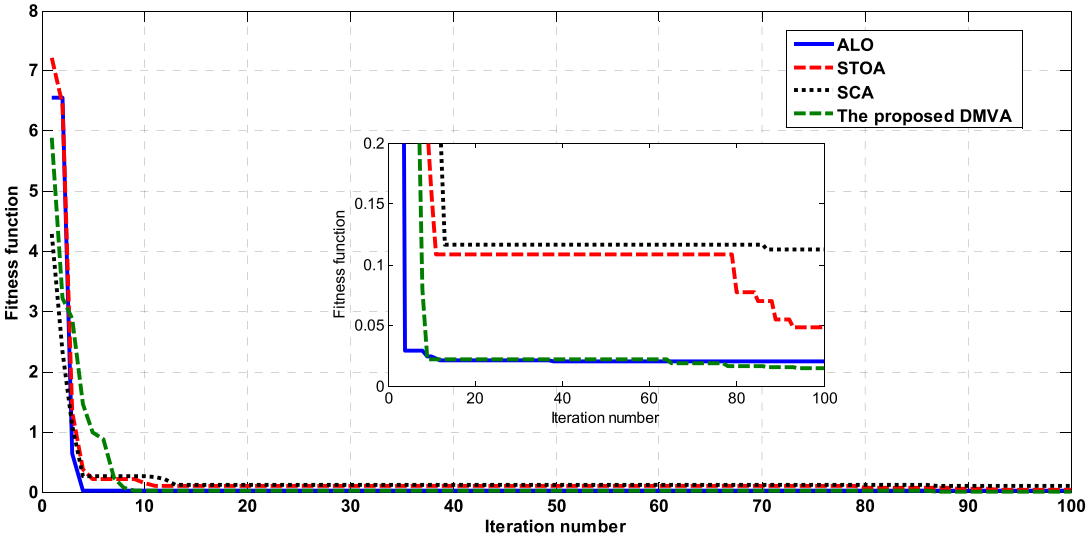

FIGURE 13. Variation of fitness function during iterative process during 1% load disturbance applied on area 1 of multi-interconnected system.

thermal, hydro, WT, PV, and nuclear. Therefore, it is important to investigate the proposed approach on system with multi-interconnected and multi-sources. This is implemented by considering four-interconnected system with PV, WT, and two thermal generating units. Moreover, the generation rate constraints (GRC) and governor dead-band (GDB) of thermal-based plant are considered. The Simulink model of the considered system is shown in Fig. 12. The first operating condition is implemented by assuming 1% load disturbance on the thermal unit located in the first area. The optimal parameters of the installed FOPID-LFC controllers obtained via the proposed approach and the others are given in Table 5, the proposed DMVA succeeded in achieving the best (minimum) fitness function of 0.015029 after the best elapsed time of 3607.9641 s. On the other hand, SCA comes in the last rank with the worst ITAE of 0.112188. regarding to the consumed time, ALO is the slowest approach as it consumes 40248.65 s.

The variations of ITAE during the iterative process for all studied optimizers are given in Fig. 13, the curves confirm the competence of the proposed approach. Moreover, the time responses of frequencies and tie-line powers' deviations in such load disturbance are given in Fig. 14, the curves confirm the superiority of the proposed DMVA compared to the others.

As the reader see, the proposed DMVA is the only algorithm which damps the oscillation of change in frequencies and tie-line powers to their steady-state values. Furthermore,

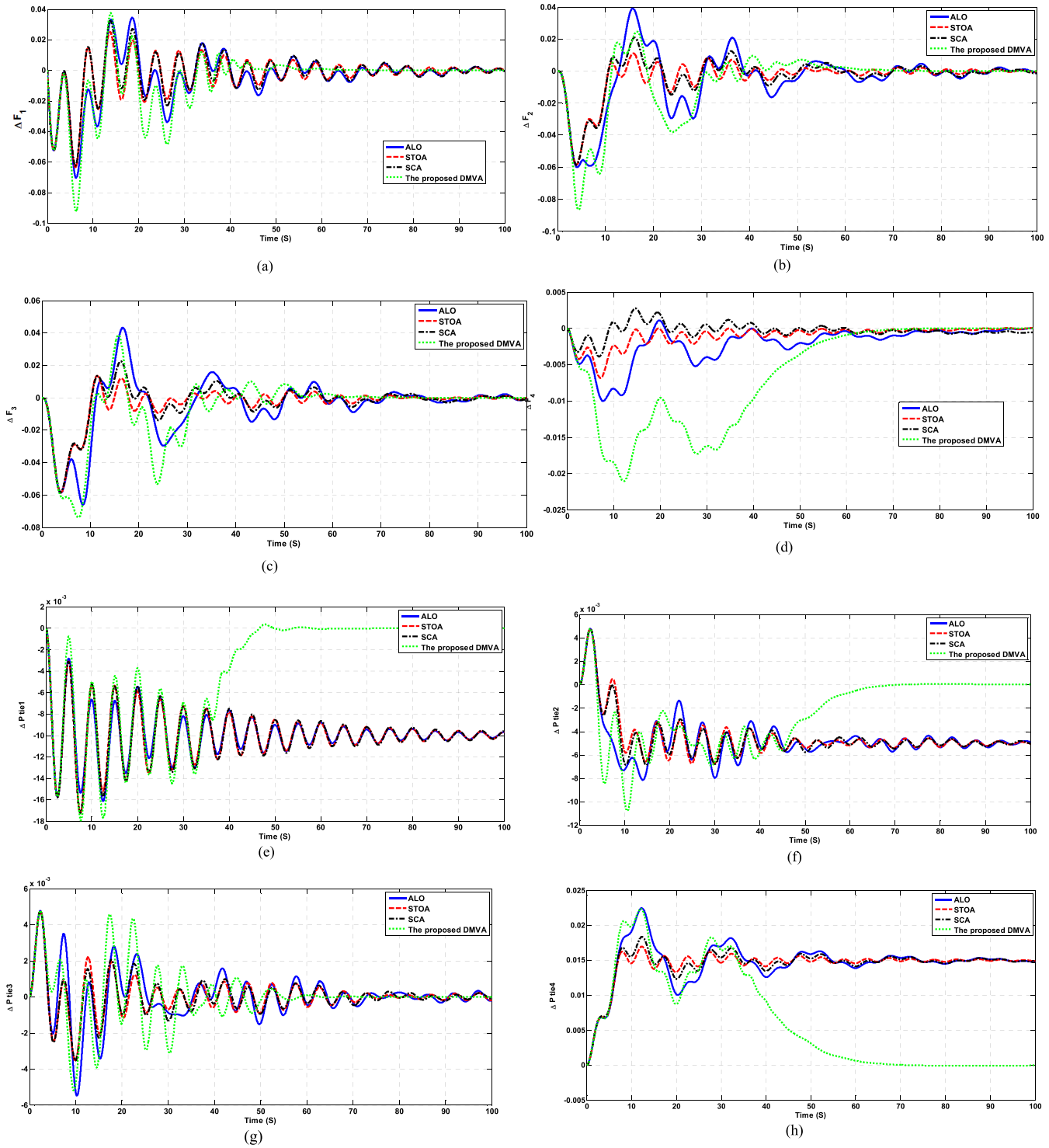

FIGURE 14. The time-responses of (a) ΔF_1, (b) ΔF_2, and (c) ΔF_3, (d) ΔF_4, (e) ΔP_{tie1}, (f) ΔP_{tie2}, (g) ΔP_{tie3}, and (h) ΔP_{tie4} for 1% load disturbance applied on area 1 of multi-interconnected system.

the rise time, settling time, minimum and maximum settling times, over shoot, under shoot, peak value, and peak time for ΔF_1, ΔF_2, ΔF_3, ΔF_4, ΔP_{tie1}, ΔP_{tie2}, ΔP_{tie3}, and ΔP_{tie4} obtained via all studied optimizers are tabulated in Table 6, the results show the reliability of the proposed approach in designing the FOPID-LFC controllers.

In order to confirm the availability of the proposed approach, second load disturbance is considered in four-interconnected system of 1% applied on area 2 which comprises WT generating unit. The proposed approach incorporated DMVA is implemented and the time responses of the frequencies and tie-line powers' deviations obtained via the

TABLE 5. The optimal parameters of FOPID controllers at 1% load disturbance applied on area 1 of multi-interconnected system.

	ALO	STOA	SCA	The proposed DMVA
K_{p1}	0.027289	0.8029	0.015345	0.68414
K_{i1}	0.012588	0.1899	0.86619	0.78884
K_{d1}	0.034782	0.01577	0.013541	1.0000
λ_1	0.027163	0.014792	0.017744	0.1959
μ_1	0.038134	0.01000	0.031131	0.24164
K_{p2}	0.18114	0.010519	0.045517	0.74218
K_{i2}	0.036437	0.016808	0.026178	1.0000
K_{d2}	0.020372	0.89511	0.059497	1.0000
λ_2	0.058786	0.012598	0.010343	0.40969
μ_2	0.016396	0.092306	0.01239	1.0000
K_{p3}	0.010749	0.014525	0.012386	0.10716
K_{i3}	0.025908	1.00000	0.50277	0.90651
K_{d3}	0.027308	0.013493	0.13517	0.093507
λ_3	0.012199	0.58147	0.01000	0.57416
μ_3	0.023182	0.019234	0.52756	1.0000
K_{p4}	0.01000	0.01214	0.024461	0.67464
K_{i4}	0.011889	0.014524	0.011453	0.00169
K_{d4}	0.2238	0.13131	0.014971	0.29009
λ_4	0.01000	0.019198	0.034235	0.029444
μ_4	0.010002	0.041136	0.14228	0.79348
Elapsed time (s)	40248.65	37506.242	38738.619	3607.9641
Fitness function	0.020613	0.048094	0.112188	0.015029

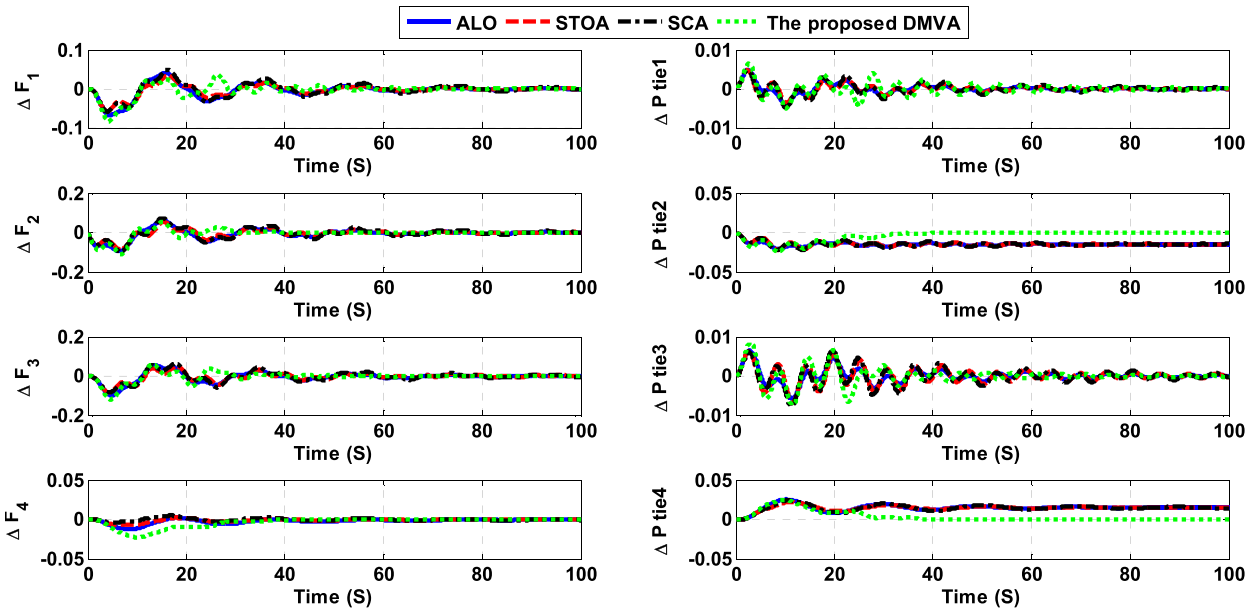

FIGURE 15. The time-responses of frequencies and tie-line powers' deviations for 1% load disturbance applied on area 2 of multi-interconnected system.

proposed approach and the others are shown in Fig. 15. It is clear that, the time responses obtained via the DMVA is the most stable compared to the others.

The proposed approach succeeded in achieving better performance in identifying the parameters of FOPID based LFC controller for multi-interconnected system operated under load disturbance on area 2.

Finally, one can derive that the proposed method surpassed the other methods that were considered in this work, as it succeeded in damping the change in frequencies and tie-line

TABLE 6. Performance specifications of frequencies and tie-line powers' deviations at 1% load disturbance applied on area 1 of multi-interconnected system.

Change in frequency of area 1 (ΔF_1)								
	t_r (s)	t_s (s)	$t_{s,min}$ (s)	$t_{s,max}$ (s)	Os (Hz)	Us (Hz)	Peak (Hz)	t_{peak} (s)
ALO	2.1732e-07	94.66849	-0.0339	0.03443	3.44367	7.0252	0.07025	6.3061
STOA	2.3222e-07	99.14593	-0.02542	0.02515	2.51472	6.3472	0.06347	6.1425
SCA	2.2897e-07	97.10739	-0.02503	0.03227	3.22717	6.25061	0.06251	6.1441
The proposed DMVA	1.7391e-07	53.36887	-0.04846	0.03760	3.76064	9.20155	0.09202	6.2874
Change in frequency of area 2 (ΔF_2)								
	t_r (s)	t_s (s)	$t_{s,min}$ (s)	$t_{s,max}$ (s)	Os (Hz)	Us (Hz)	Peak (Hz)	t_{peak} (s)
ALO	6.6950e-07	93.4864	-0.02965	0.03903	3.9025	6.00474	0.0600	4.0892
STOA	5.8223e-07	84.8654	-0.01337	0.01104	1.1044	5.86164	0.0586	3.9331
SCA	4.9326e-07	86.5567	-0.01474	0.02092	2.0923	5.85119	0.05851	3.9311
The proposed DMVA	2.8386e-07	61.1885	-0.03810	0.02469	2.4685	8.65873	0.08659	4.3591
Change in tie-line power (ΔF_3)								
	t_r (s)	t_s (s)	$t_{s,min}$ (s)	$t_{s,max}$ (s)	Os (Hz)	Us (Hz)	Peak (Hz)	t_{peak} (s)
ALO	3.6793e-07	99.0772	-0.02962	0.04326	4.3260	6.5968	0.06596	8.5262
STOA	4.0029e-07	72.4453	-0.00939	0.01349	1.3486	5.8599	0.05859	3.9331
SCA	4.0404e-07	99.7377	-0.01398	0.02259	2.2588	5.84193	0.05842	3.9207
The proposed DMVA	7.4094e-07	60.4535	-0.05317	0.03862	3.8615	7.40504	0.07405	7.5705
Change in tie-line power (ΔF_4)								
	t_r (s)	t_s (s)	$t_{s,min}$ (s)	$t_{s,max}$ (s)	Os (Hz)	Us (Hz)	Peak (Hz)	t_{peak} (s)
ALO	4.9424e-06	93.5871	-0.00520	0.00109	0.10886	1.00078	0.01001	7.72611
STOA	0.00011	92.6676	-0.00015	6.83623e-05	0.00684	0.68249	0.00682	7.16904
SCA	4.2776e-06	85.8878	-0.00119	0.00277	0.27718	0.38798	0.00388	6.90500
The proposed DMVA	0.0019	64.8963	1.82172e-08	1.20117e-05	0.001200	2.105629	0.02106	12.1738
Change in tie-line power (ΔP_{tie1})								
	t_r (s)	t_s (s)	$t_{s,min}$ (s)	$t_{s,max}$ (s)	Os (Hz)	Us (Hz)	Peak (Hz)	t_{peak} (s)
ALO	0.94293	99.01328	-0.016135	-0.002830	6.643e-07	0.0000	0.01614	12.4995
STOA	0.94168	99.09647	-0.017267	-0.003119	7.832e-07	0.0000	0.01727	7.52664
SCA	0.93544	99.24669	-0.017249	-0.003153	7.956e-07	0.0000	0.01725	7.52878
The proposed DMVA	0.02081	45.84533	-0.000196	0.0003500	2.698e-05	0.0014	0.01793	7.62024
Change in tie-line power (ΔP_{tie2})								
	t_r (s)	t_s (s)	$t_{s,min}$ (s)	$t_{s,max}$ (s)	Os (Hz)	Us (Hz)	Peak (Hz)	t_{peak} (s)
ALO	2.51390	96.8766	-0.00815	-0.00136	6.689e-07	9.764e-07	0.00815	14.0128
STOA	5.13858	88.4708	-0.00673	-0.00309	3.396e-07	9.479e-07	0.00674	24.8454
SCA	4.85084	98.4323	-0.00688	-0.00294	3.692e-07	9.470e-07	0.00688	14.8003
The proposed DMVA	0.05507	64.8301	-0.01079	0.004761	0.000296	0.000673	0.01079	10.5474
Change in tie-line power (ΔP_{tie3})								
	t_r (s)	t_s (s)	$t_{s,min}$ (s)	$t_{s,max}$ (s)	Os (Hz)	Us (Hz)	Peak (Hz)	t_{peak} (s)
ALO	0.04789	98.98913	-0.00548	0.00349	2.454e-05	2.221e-05	0.00548	10.28495
STOA	0.04007	98.99859	-0.00355	0.00220	1.785e-05	2.531e-05	0.00477	2.358965
SCA	0.02026	99.07223	-0.00354	0.00207	3.552e-05	4.913e-05	0.00476	2.357854
The proposed DMVA	0.00444	60.87266	-0.00519	0.00477	0.06426	0.07011	0.00519	9.585309
Change in tie-line power (ΔP_{tie4})								
	t_r (s)	t_s (s)	$t_{s,min}$ (s)	$t_{s,max}$ (s)	Os (Hz)	Us (Hz)	Peak (Hz)	t_{peak} (s)
ALO	5.57367	93.3337	0.01003	0.022465	5.186e-07	0.0000	0.02246	12.26386
STOA	5.63798	72.7505	0.01329	0.016993	1.405e-07	0.0000	0.01699	12.32372
SCA	5.52224	93.7517	0.01233	0.018366	2.467e-07	0.0000	0.01837	12.35219
The proposed DMVA	1.94465	62.1615	-5.8107e-05	-2.5785e-05	1.031e-06	0.00078	0.02238	12.09054

powers between the interconnected plants to their steady-state values in all the cases studied.

VI. CONCLUSION

This paper proposes a fractional-order PID (FOPID) based LFC controller installed in multi-interconnected system with renewable energy-based plants. The installed controller is designed with the aid of new methodology incorporated movable damped wave algorithm (MDVA) via determining its optimal parameters. The considered fitness function to be minimized is the integral time absolute error (ITAE) of the frequencies and tie-line powers' violations. The designed LFC is installed in different systems, the first one is two-interconnected system with PV and thermal generating units while the second one has four plants, PV, WT, and two thermal units with GRC and GDB. Different load

disturbances are considered in both constructed systems. Moreover, comparison to coronavirus herd immunity optimizer (CHIO), antlion optimizer (ALO), sooty tern optimization algorithm (STOA), manta ray foraging optimizer (MRFO), and sin-cos algorithm (SCA) is conducted. Furthermore, statistical analysis is conducted by calculating the best, worst, mean, median, variance, and standard deviation after several runs of each optimizer. Additionally, the performance specifications of the time responses of frequencies and tie-line powers' violations are calculated.

Regarding to the first considered system, in case of applying 10% load disturbance on the PV plant, the proposed DMVA succeeded in achieving the best ITAE of 6.3911. On the other hand, MRFO achieved the second rank with fitness function of 6.9375 and CHIO came in the last rank with the worst ITAE of 8.6836. Other errors, IAE, ISE, and ITSE, are calculated in such case, the proposed DMVA achieved the best values of 5.9883, 0.1238, and 0.0312 for the stated errors respectively. While SCA came in the second rank achieving errors of 6.0948, 0.1236, and 0.0318. Regarding to the statistical parameters, the best variance and standard deviation of 0.0279 and 0.1672 are obtained via the proposed DMVA while the worst values are 15631.25 and 125.0250 obtained via CHIO. In the second load disturbance of 10% applied on thermal based plant, the proposed approach achieved the best fitness function of 1.205898, the next one is STOA with ITAE of 6.81865. Regarding to the multi-interconnected system, when applying a load disturbance of 1% on the first thermal plant, the proposed DMVA succeeded in achieving the best (minimum) fitness function of 0.015029 after the best elapsed time of 3607.9641 s. The obtained results confirmed the robustness and competence of the proposed approach in identifying the optimal parameters of FOPID based LFC installed in multi-interconnected system with renewable energy-based plants. The authors recommended modification in DMVA to enhance its convergence speed in the future work. Moreover, expansion of the constructed interconnected system with more penetration of renewable energy sources is also recommended.

ACKNOWLEDGMENT

The authors would like to thank their sincere appreciation to the Central Laboratory at Al-Jouf University for support this study.

REFERENCES

[1] W. Zhang and K. Fang, "Controlling active power of wind farms to participate in load frequency control of power systems," *IET Gener., Transmiss. Distrib.*, vol. 11, no. 9, pp. 2194–2203, Jun. 2017.
[2] Y. Xu, C. Li, Z. Wang, N. Zhang, and B. Peng, "Load frequency control of a novel renewable energy integrated micro-grid containing pumped hydropower energy storage," *IEEE Access*, vol. 6, pp. 29067–29077, 2018.
[3] D. H. Tungadio and Y. Sun, "Load frequency controllers considering renewable energy integration in power system," *Energy Rep.*, vol. 5, pp. 436–453, Nov. 2019.
[4] D. Yousri, T. S. Babu, and A. Fathy, "Recent methodology based harris hawks optimizer for designing load frequency control incorporated in multi-interconnected renewable energy plants," *Sustain. Energy, Grids Netw.*, vol. 22, Jun. 2020, Art. no. 100352.
[5] Z. Yan and Y. Xu, "Data-driven load frequency control for stochastic power systems: A deep reinforcement learning method with continuous action search," *IEEE Trans. Power Syst.*, vol. 34, no. 2, pp. 1653–1656, Mar. 2019.
[6] H. Amano, Y. Ohshiro, T. Kawakami, and T. Inoue, "Utilization of battery energy storage system for load frequency control toward large-scale renewable energy penetration," in *Proc. 3rd IEEE PES Innov. Smart Grid Technol. Eur. (ISGT Europe)*, Oct. 2012, pp. 1–7.
[7] A. Datta, K. Bhattacharjee, S. Debbarma, and B. Kar, "Load frequency control of a renewable energy sources based hybrid system," in *Proc. IEEE Conf. Syst., Process Control (ICSPC)*, Dec. 2015, pp. 34–38.
[8] J. Yang, Z. Zeng, Y. Tang, J. Yan, H. He, and Y. Wu, "Load frequency control in isolated micro-grids with electrical vehicles based on multivariable generalized predictive theory," *Energies*, vol. 8, no. 3, pp. 2145–2164, Mar. 2015.
[9] R. Ali, T. H. Mohamed, Y. S. Qudaih, and Y. Mitani, "A new load frequency control approach in an isolated small power systems using coefficient diagram method," *Int. J. Electr. Power Energy Syst.*, vol. 56, pp. 110–116, Mar. 2014.
[10] S. Trip and C. De Persis, "Distributed optimal load frequency control with non-passive dynamics," *IEEE Trans. Control Netw. Syst.*, vol. 5, no. 3, pp. 1232–1244, Sep. 2018.
[11] M.-H. Khooban, T. Niknam, M. Shasadeghi, T. Dragicevic, and F. Blaabjerg, "Load frequency control in microgrids based on a stochastic noninteger controller," *IEEE Trans. Sustain. Energy*, vol. 9, no. 2, pp. 853–861, Apr. 2018.
[12] E. Çam, "Application of fuzzy logic for load frequency control of hydroelectrical power plants," *Energy Convers. Manage.*, vol. 48, no. 4, pp. 1281–1288, Apr. 2007.
[13] A. Safari, F. Babaei, and M. Farrokhifar, "A load frequency control using a PSO-based ANN for micro-grids in the presence of electric vehicles," *Int. J. Ambient Energy*, vol. 42, no. 6, pp. 688–700, Apr. 2021.
[14] Y. Mi, X. Hao, Y. Liu, Y. Fu, C. Wang, P. Wang, and P. C. Loh, "Sliding mode load frequency control for multi-area time-delay power system with wind power integration," *IET Gener., Transmiss. Distrib.*, vol. 11, no. 18, pp. 4644–4653, 2017.
[15] C. Mu, Y. Tang, and H. He, "Improved sliding mode design for load frequency control of power system integrated an adaptive learning strategy," *IEEE Trans. Ind. Electron.*, vol. 64, no. 8, pp. 6742–6751, Aug. 2017.
[16] M. Dreidy, H. Mokhlis, and S. Mekhilef, "Inertia response and frequency control techniques for renewable energy sources: A review," *Renew. Sustain. Energy Rev.*, vol. 69, pp. 144–155, Mar. 2017.
[17] D. Yu, H. Zhu, W. Han, and D. Holburn, "Dynamic multi agent-based management and load frequency control of PV/fuel cell/wind turbine/CHP in autonomous microgrid system," *Energy*, vol. 173, pp. 554–568, Apr. 2019.
[18] G. Shahgholian, "Power system stabilizer application for load frequency control in hydro-electric power plant," *Int. J. Theor. Appl. Math.*, vol. 3, no. 4, pp. 148–157, 2017.
[19] A. Pappachen and A. Peer Fathima, "Critical research areas on load frequency control issues in a deregulated power system: A state-of-the-art-of-review," *Renew. Sustain. Energy Rev.*, vol. 72, pp. 163–177, May 2017.
[20] M.-H. Khooban, "Secondary load frequency control of time-delay standalone microgrids with electric vehicles," *IEEE Trans. Ind. Electron.*, vol. 65, no. 9, pp. 7416–7422, Sep. 2018.
[21] V. Gholamrezaie, M. G. Dozein, H. Monsef, and B. Wu, "An optimal frequency control method through a dynamic load frequency control (LFC) model incorporating wind farm," *IEEE Syst. J.*, vol. 12, no. 1, pp. 392–401, Mar. 2018.
[22] M. Hajiakbari Fini and M. E. Hamedani Golshan, "Determining optimal virtual inertia and frequency control parameters to preserve the frequency stability in islanded microgrids with high penetration of renewables," *Electr. Power Syst. Res.*, vol. 154, pp. 13–22, Jan. 2018.
[23] K. Liao and Y. Xu, "A robust load frequency control scheme for power systems based on second-order sliding mode and extended disturbance observer," *IEEE Trans. Ind. Informat.*, vol. 14, no. 7, pp. 3076–3086, Jul. 2018.
[24] H. H. Alhelou, M. E. Hamedani-Golshan, E. Heydarian-Forushani, A. S. Al-Sumaiti, and P. Siano, "Decentralized fractional order control scheme for LFC of deregulated nonlinear power systems in presence of EVs and RER," in *Proc. Int. Conf. Smart Energy Syst. Technol. (SEST)*, Sep. 2018, pp. 1–6.
[25] K. S. Ko and D. K. Sung, "The effect of EV aggregators with time-varying delays on the stability of a load frequency control system," *IEEE Trans. Power Syst.*, vol. 33, no. 1, pp. 669–680, Jan. 2018.

[26] H. M. Hasanien, "Whale optimisation algorithm for automatic generation control of interconnected modern power systems including renewable energy sources," *IET Gener., Transmiss. Distrib.*, vol. 12, no. 3, pp. 607–614, Feb. 2018.
[27] H. H. Ali, A. Fathy, and A. M. Kassem, "Optimal model predictive control for LFC of multi-interconnected plants comprising renewable energy sources based on recent sooty terns approach," *Sustain. Energy Technol. Assessments*, vol. 42, Dec. 2020, Art. no. 100844.
[28] H. H. Ali, A. M. Kassem, M. Al-Dhaifallah, and A. Fathy, "Multi-verse optimizer for model predictive load frequency control of hybrid multi-interconnected plants comprising renewable energy," *IEEE Access*, vol. 8, pp. 114623–114642, 2020.
[29] A. Fathy, A. M. Kassem, and A. Y. Abdelaziz, "Optimal design of fuzzy PID controller for deregulated LFC of multi-area power system via mine blast algorithm," *Neural Comput. Appl.*, vol. 32, no. 9, pp. 4531–4551, May 2020.
[30] A. Fathy and A. M. Kassem, "Antlion optimizer-ANFIS load frequency control for multi-interconnected plants comprising photovoltaic and wind turbine," *ISA Trans.*, vol. 87, pp. 282–296, Apr. 2019.
[31] A. Prakash and S. K. Parida, "LQR based PI controller for load frequency control with distributed generations," in *Proc. 21st Nat. Power Syst. Conf. (NPSC)*, Dec. 2020, pp. 1–5.
[32] A. Prakash, K. Kumar, and S. K. Parida, "PIDF (1+ FOD) controller for load frequency control with SSSC and AC–DC tie-line in deregulated environment," *IET Gener., Transmiss. Distrib.*, vol. 14, no. 14, pp. 2751–2762, 2020.
[33] A. Datta, I. Koley, G. K. Panda, A. C. Atoche, and J. V. Castillo, "Dynamic power–frequency control in a hybrid wind-PV plant interlinked with AC power system," *J. Elect. Eng. Technol.*, vol. 16, pp. 1469–1479, Mar. 2021.
[34] R. K. Khadanga, A. Kumar, and S. Panda, "A novel sine augmented scaled sine cosine algorithm for frequency control issues of a hybrid distributed two-area power system," *Neural Comput. Appl.*, early access, pp. 1–14, 2021, doi: 10.1007/s00521-021-05923-w.
[35] E. M. Ahmed, E. A. Mohamed, A. Elmelegi, M. Aly, and O. Elbaksawi, "Optimum modified fractional order controller for future electric vehicles and renewable energy-based interconnected power systems," *IEEE Access*, vol. 9, pp. 29993–30010, 2021.
[36] R. K. Khadanga, A. Kumar, and S. Panda, "Frequency control in hybrid distributed power systems via type-2 fuzzy PID controller," *IET Renew. Power Gener.*, early access, doi: 10.1049/rpg2.12140.
[37] M. Barakat, A. Donkol, H. F. A. Hamed, and G. M. Salama, "Harris hawks-based optimization algorithm for automatic LFC of the interconnected power system using PD-PI cascade control," *J. Elect. Eng. Technol.*, early access, pp. 1–21, 2021, doi: 10.1007/s42835-021-00729-1.
[38] C. Zhang, S. Wang, and Q. Zhao, "Distributed economic MPC for LFC of multi-area power system with wind power plants in power market environment," *Int. J. Electr. Power Energy Syst.*, vol. 126, Mar. 2021, Art. no. 106548.
[39] P. C. Pradhan, R. K. Sahu, and S. Panda, "Analysis of hybrid fuzzy logic control based PID through the filter for frequency regulation of electrical power system with real-time simulation," *J. Control, Autom. Electr. Syst.*, vol. 32, no. 2, pp. 439–457, Apr. 2021.
[40] M. Sharma, S. Dhundhara, S. Singh, and Y. P. Verma, "Multi-verse optimizer based fuzzy-PI controller for robust frequency regulation in thermal-hydro power system," in *Proc. IOP Conf., Mater. Sci. Eng.*, 2021, vol. 1033, no. 1, Art. no. 012033.
[41] Y. Arya, "Effect of electric vehicles on load frequency control in interconnected thermal and hydrothermal power systems utilising CF-FOIDF controller," *IET Gener., Transmiss. Distrib.*, vol. 14, no. 14, pp. 2666–2675, 2020.
[42] T. Santy and R. Natesan, "Load frequency control of a two area hybrid system consisting of a grid connected PV system and thermal generator," *Int. J. Emerg. Technol. Comput. Electron*, vol. 13, no. 1, pp. 456–461, no. 2015.
[43] H. Renaudineau, F. Donatantonio, J. Fontchastagner, G. Petrone, G. Spagnuolo, J.-P. Martin, and S. Pierfederici, "A PSO-based global MPPT technique for distributed PV power generation," *IEEE Trans. Ind. Electron.*, vol. 62, no. 2, pp. 1047–1058, Feb. 2015.
[44] S. Adhikari and F. Li, "Coordinated V-f and P-Q control of solar photovoltaic generators with MPPT and battery storage in microgrids," *IEEE Trans. Smart Grid*, vol. 5, no. 3, pp. 1270–1281, May 2014.
[45] M. Adly and A. H. Besheer, "A meta-heuristics search algorithm as a solution for energy transfer maximization in stand-alone photovoltaic systems," *Int. J. Electr. Power Energy Syst.*, vol. 51, pp. 243–254, Oct. 2013.
[46] M. K. Alam and F. H. Khan, "Transfer function mapping for a grid connected PV system using reverse synthesis technique," in *Proc. IEEE 14th Workshop Control Modeling Power Electron. (COMPEL)*, Jun. 2013, pp. 1–5.
[47] A. M. Kassem and A. Y. Abdelaziz, "Reactive power control for voltage stability of standalone hybrid wind–diesel power system based on functional model predictive control," *IET Renew. Power Gener.*, vol. 8, no. 8, pp. 887–899, 2014.
[48] A. M. Kassem and A. M. Yousef, "Voltage and frequency control of an autonomous hybrid generation system based on linear model predictive control," *Sustain. Energy Technol. Assessments*, vol. 4, pp. 52–61, Dec. 2013.
[49] S. Chekkal, N. A. Lahaçani, D. Aouzellag, and K. Ghedamsi, "Fuzzy logic control strategy of wind generator based on the dual-stator induction generator," *Int. J. Electr. Power Energy Syst.*, vol. 59, pp. 166–175, Jul. 2014.
[50] I. Podlubny, "Fractional-order systems and fractional-order controllers," *Inst. Exp. Phys., Slovak Acad. Sci., Kosice*, vol. 12, no. 3, pp. 1–18, 1994.
[51] R. M. Rizk-Allah and A. E. Hassanien, "A movable damped wave algorithm for solving global optimization problems," *Evol. Intell.*, vol. 12, no. 1, pp. 49–72, Mar. 2019.

AHMED FATHY received the B.Sc. (Hons.), M.Sc., and Ph.D. degrees in electrical engineering from Zagazig University, Egypt, in 2006, 2009, and 2014, respectively. Since January 2014, he has been working as an Assistant Professor with the Electric Power and Machines Department, Zagazig University. In February 2019, he has the scientific title of an Associate Professor with degree of scientific excellence. He is currently an Assistant Professor with the Electrical Engineering Department, Faculty of Engineering, Jouf University, Saudi Arabia. He has authored or coauthored more than 60 refereed journal articles and conference papers. His research interests include renewable energy optimization, optimal location of DGs in distribution networks, LFC, design of maximum power point trackers, applications of AI, and optimization techniques. He has been awarded many prizes for distinct research and international publishing from Zagazig University.

ABDULLAH G. ALHARBI (Member, IEEE) received the B.Sc. degree in electronics and communications engineering from Qassim University, Saudi Arabia, in 2010, and the master's and Ph.D. degrees in electrical engineering from the University of Missouri–Kansas City, USA, in 2014 and 2017, respectively. From 2010 to 2012, he was an Electrical Engineer with Saudi Aramco Company. He is currently an Assistant Professor with the Electrical Engineering Department, Jouf University, Saudi Arabia. He has authored and coauthored over 45 journal articles and conference papers and one Springer book chapter. His research interests include digital IC design, memristor-based circuits, traffic engineering, cloud computing, and network routing. He is also a member of the Gulf Engineering Union, the IEEE Circuits and Systems Society, the IEEE Young Professionals, the IEEE Signal Processing Society, the IEEE Instrumentation and Measurement Society Membership, and the IEEE Communications Society Membership; and a Professional Member of ACM. He was a recipient of several awards from Saudi Arabian Cultural Mission, USA, and the University of Missouri–Kansas City.